

STRONG MAGNETIC FIELD GRADIENTS FOR HIGH RESOLUTION
NUCLEAR MAGNETIC RESONANCE IMAGING

by

Yisa S. Rumala

Thesis

Submitted in partial fulfillment of the requirements for the degree of

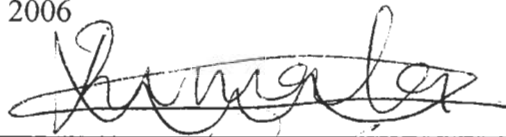
Bachelors with Honors in Physics and Mathematics

at

York College of The City University of New York

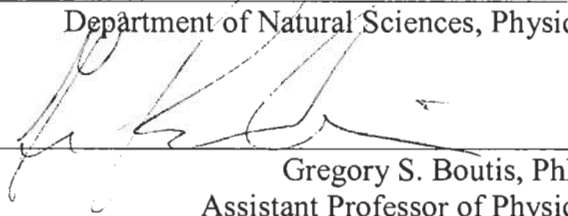
June 2006

Author



Department of Natural Sciences, Physics

Advisor



Gregory S. Boutis, PhD
Assistant Professor of Physics

Physics Coordinator Signature



D. C. Jain, PhD
Professor of Physics

Chairman of The Natural Sciences Department



Lawrence W. Johnson, PhD
Professor of Chemistry

Abstract

In Nuclear Magnetic Resonance, a strong pulsed gradient field can be used to significantly improve the imaging resolution in microscopy experiments. This thesis details an analysis to generate pulsed gradient fields on the order of 400, 000G/cm over a sample volume of one cubic millimeter, while minimizing adverse effects such as joule's heating, inductance and higher terms of the magnetic field expansion. These gradient fields are at least 1 order of magnitude greater than that previously reported and approximately 4 orders of magnitude greater than what is commercially available. The gradient fields will be used to perform high resolution studies of a broad range of materials in the NMR laboratory at York College, which includes investigating the structure of biological samples such as elastin and fruit cuticles as well as applications to investigating quantum dynamics in homogenous solids.

Acknowledgements

First of all, I would like to thank my advisor, Professor Gregory Boutis, for giving me the opportunity to embark on NMR research in his group, and also for his guidance and support while I worked on the various projects in the lab. Learning about gradient coils and how to apply quantum mechanics to problems in NMR research has truly broadened my scientific horizons. Special thanks to Dr Eugene Mananga, and Rabia Roopchand for many enlightening discussions. You people are great colleagues and friends!

Second, I would like to thank my past advisors, Professor Claire Gmachl (Princeton University), Professor Farley Mawyer (Dept. of Math and Comp. Studies, York College), and Professor Martin Culpepper (MIT), for initially exposing me to the research methodology, and giving me the opportunity to get my feet wet in the research world. Third, I would like to thank the financial support from the Carver Bancorp scholarship program, the NSF sponsored New York City LSAMP research assistantship scholarship program, and the Department of Education Ronald E. McNair Scholars program. Through participation in these programs I have met many brilliant colleagues as well as professionals in the field.

Fourth, I would like to thank my uncle Mr Sode-Shinni Rumala for believing in me during my very early years of development. Finally, I would like to thank my parents and siblings for their enormous love and hard work which has enabled me to reach the point I am today.

Table of Contents:

1. Introduction	5
2. Larmor equation to show how improved resolution is obtained	6
3. k space and q- space imaging	7
4. Magnetic field gradient for a single Maxwell pair	11
5. Generating a linear gradient field using multiple Maxwell pairs	13
6. Inductance of a gradient coil	14
7. Parameters used in this design	15
8. Conclusion	18
9. List of Appendices	19
a) Cross sectional view for gradient dimensions	
b) Picture of an NMR assembly	
c) Picture of what the gradient set will look like	
10. References	22

Strong Magnetic Field Gradients for High Resolution Nuclear Magnetic Resonance

Imaging

Introduction

One application of an NMR gradient coil is to generate a spatially varying magnetic field for image creation. It was first demonstrated by Paul Lauterbur in a 1973 ground breaking paper published in Nature. He showed that by adding a linear magnetic field gradient to a homogenous magnetic field, a 2D image of two glass tubes with normal water (within a larger container of deuterated water) could be obtained from the signal distribution. Lauterbur termed this technique as zeugmatography (from Greek ζευγμα meaning “that which is used for”) [1], and later won the 2003 Nobel Prize in medicine for this work. This concept has been further developed into more sophisticated coil configurations for better functionality. Such configurations have been quite successful in various areas of NMR research such as in medical imaging, and studying the structure and dynamics (chemical dynamics, quantum dynamics etc) of various processes in the solid and liquid state [2, 3].

As NMR instrumentation research continues to advance, there is an ever increasing demand to create higher resolution images which would enable high precision experiments such as investigating diffusion in porous and amorphous systems. Most NMR imaging apparatus are limited [4, 5, 16] in creating such fine resolution images due to the particular imaging methodology (k space or q space imaging techniques), and the sample size (with smaller sample sizes, a stronger gradient can be generated). One way of overcoming this problem is by utilizing very strong gradients [3] which may enable submicron resolution in the nanometer scale.

Larmor equation to show how improved resolution is obtained

The Larmor equation is a basic equation in NMR. It relates the resonant frequency of a nucleus to the magnetic field, and it is represented as:

$$\omega = \gamma B \quad (1)$$

ω , γ and B are the resonant frequency, gyromagnetic ratio, and static homogenous magnetic field, respectively [6]. By having a magnetic field gradient superimposed on the homogenous magnetic field (equation below), the spatial position of the nucleus in a sample can be obtained by varying the nuclei's resonant frequency.

$$\omega_i(z) = \gamma B + \gamma \frac{\partial B}{\partial z} z_i \quad (2)$$

where $\omega_i(z)$ is the resonant frequency of the i_{th} nucleus, γ is the gyromagnetic ratio, B is the static magnetic field, $\frac{\partial B}{\partial z}$ is the magnetic field gradient and z_i is the position of the i_{th} nucleus. This equation could be used to show how the resolution of the resulting image is enhanced with larger field gradients. The concept is illustrated by plotting a graph of the frequency of the i_{th} nucleus as a function of its position where the gradient field is increased. Figure 1 makes use of just two atomic nuclei spin, but realistically there is an Avogadro number of nuclear spins in a sample.

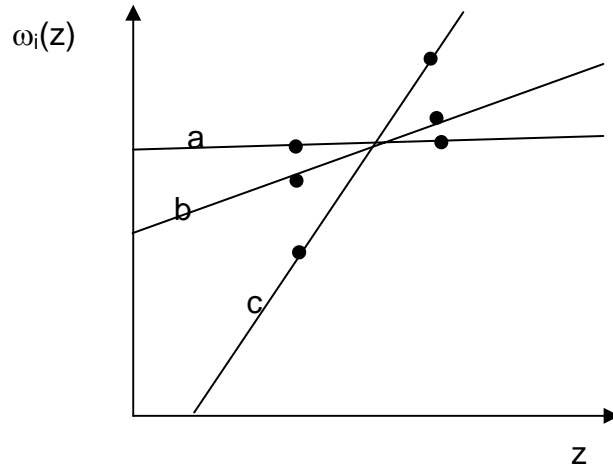


Figure 1: The two dots represent 2 atomic nuclei. (a) When there is no magnetic field gradient, the two nuclei are resonating at the same frequency and cannot be distinguished. (b) When a magnetic field gradient is imposed, the two nuclei are resonating at slightly different frequencies, and therefore can be distinguished. (c) With a higher gradient, the resonating frequency difference between the nuclei is better differentiated leading to better imaging resolution of the sample.

From figure 1, one can note that as the magnetic field gradient is increased, the difference in resonating frequency between the individual nuclei is larger, which results in better imaging resolution. This is because the resolution of an image is determined by how well one can distinguish the frequency of one point (or nucleus) on the sample from another point on the sample. Neglecting molecular displacements, if two points on a sample can be distinguished well enough when measuring the density of spins, the image obtained will be improved.

k-space and q-space imaging

k-space imaging

There are two major types of imaging schemes that can be used during NMR microscopy experiments. The first is k-space imaging and the other is q space imaging. k-space imaging measures the density of nuclear spins over a sample

volume, and the limits of resolution are dictated by the gradient field strengths, and molecular diffusion in the sample. A brief mathematical description of a one dimensional k-space imaging scheme is described below [7, 3]. In what follows, it is assumed that there is no relaxation or diffusion within the sample.

Pulse sequence:

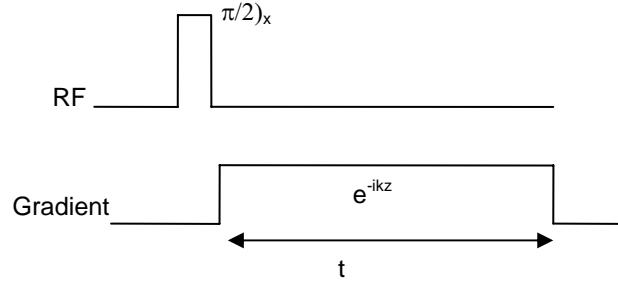


Figure 2: shows a $\pi/2$ radio frequency (RF) pulse applied about the x axis with no gradient, and then a gradient pulse of time t is applied to the system.

Without a gradient the spin density ρ with magnization M over a sample volume of V is given by

$$\rho = \frac{M}{V} \quad (3)$$

If the magnetization M varies as a function of z , ρ will vary as a function of z .

The signal deduced over a sample volume is given by

$$Signal = \int \rho(z) dV \quad (4)$$

where dV (e.g. $dx dy dz$) is the volume element, but since we will be talking about a 1D image, the volume element will be dz .

When a gradient is applied, the signal is

$$Signal(t) = \int \rho(z) e^{ikz} dz \quad (5)$$

Where $k = \gamma \frac{\partial B}{\partial z} t$, and γ , t , $\frac{\partial B}{\partial z}$ are the gyromagnetic ratio, pulse time, and gradient strength, respectively. The density of the spins is deduced from the inverse Fourier transform of the of the signal and it is represented as

$$\rho(z) = \int \text{Signal}(t) e^{-ikt} dt \quad (6)$$

The major factor that causes blurring of the image during k-space imaging is diffusion. This is attributed to the random motions of the molecules while the spin density is measured which broadens the line shape of the signal.

q-space imaging

q-space imaging measures the average probability of molecular displacements of molecules. The limits of resolution are dictated by how well one can reproduce the gradient pulse areas, and the pulse gradient strengths. A brief mathematical description of this imaging scheme is shown as well [7, 3]. In what follows, it is assumed that there is no relaxation of the spins in the sample.

Pulse sequence

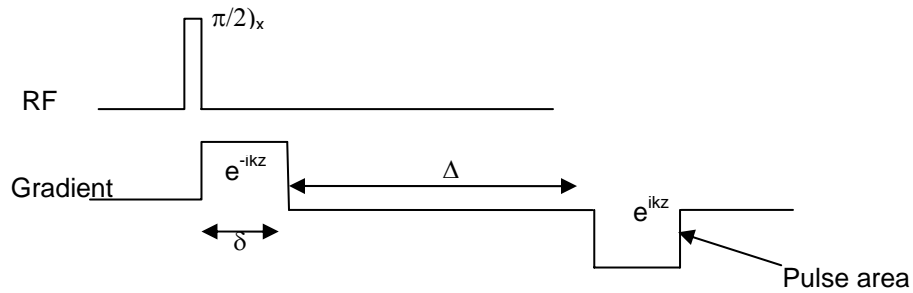


Figure 3: shows a $\pi/2$ radio frequency (RF) pulse about the x axis under no gradient, and then a positive area gradient is applied for a time duration δ after which the spins is allowed to diffuse for a time Δ before a negative area gradient pulse is applied. It should be noted that $\Delta \gg \delta$, and diffusion during δ is negligible.

Without a gradient, the signal is represented by the below integral which is the same as in k-space imaging.

$$Signal(t) = \int \rho(z)e^{ikz} dz \quad (7)$$

With the gradient pulse scheme shown in figure 3, the signal as a function of time is

$$Signal(\delta) = \iint \rho(z) e^{-ikz} P(z'|z, \Delta) e^{ikz'} dz dz' \quad (8)$$

Where $k = \gamma \frac{\partial B}{\partial z} \delta$, and γ , δ , $\frac{\partial B}{\partial z}$, are the gyromagnetic ratio, pulse time, gradient strength, respectively. $P(z'|z, \Delta)$ is the notation for the conditional probability that a spin at position z' moves to z in time Δ . In the case of free diffusion, $P(z'|z, \Delta)$ is a Gaussian, while in the case of bound diffusion, $P(z'|z, \Delta)$ depends on the geometry of the pores that the water is confined to and other variables. By performing a change of variable to equation 8, the integral can be written as

$$Signal(\delta) = \int \rho(R, \Delta) e^{ikR} dR \quad (9)$$

where $R = z' - z$ and $\rho(R, \Delta) = \rho(z) P(z'|z, \Delta)$.

One can combine gradient pulses in different sequences by varying the pulse time (t as in k-space imaging or δ as in q-space imaging), or varying the gradient field strength to improve resolution of the resulting image.

Magnetic field gradient for a single Maxwell pair

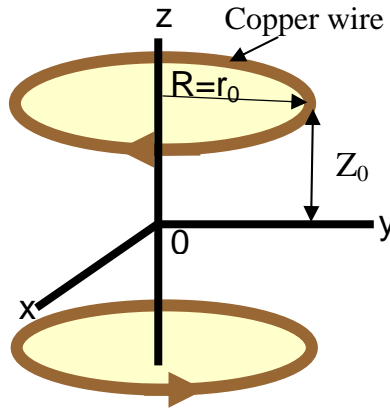


Figure 4: shows a single Maxwell pair configuration of radius R , and distance from the copper wire to center of the loops Z_0

A simple configuration for generating a magnetic field gradient can be achieved by using a pair of Maxwell coils, as shown in figure 4. When a current is applied in opposite directions through the individual loops of copper wire, a magnetic field is created in opposite directions. At the center of the loops the two fields cancel out to form a zero magnetic field, and as one moves towards either loop the field increases, thus forming a gradient field. The gradient for a Maxwell pair with radii r_0 , centered at $z = \pm z_0$ can be deduced from Biot-Savart law [8], and it is indicated below:

$$B(r) = \frac{\mu I}{4\pi} \int \frac{dl \times \hat{r}}{r^2} \quad (\text{Biot-Savart law}) \quad (10)$$

Performing a change of variable, and differentiating the integral, the equation may be written as [9]

$$\frac{\partial B(r, z)}{\partial z} = \frac{3\mu I r_0}{4\pi} \int_0^{2\pi} d\phi' (r_0 - r \cos \phi') \times \left\{ \frac{z_0 - z}{\left[r^2 + r_0^2 - 2rr_0 \cos \phi' + (z_0 - z)^2 \right]^{5/2}} + \frac{z_0 + z}{\left[r^2 + r_0^2 - 2rr_0 \cos \phi' + (z_0 + z)^2 \right]^{5/2}} \right\} \quad (11)$$

Upon evaluating the integral, the gradient at the center of a single Maxwell pair is

$$\frac{\partial B}{\partial z} \Big|_{z=0} = \frac{3z\mu I}{\left(1 + \left(\frac{z_0}{R} \right)^2 \right)^{\frac{5}{2}} R^3} \quad (12)$$

where z_0 is the distance from one loop to the center, μ_0 is the permeability of free space, I is the current flowing through the loop and R is the radius of the loop. A symbolic software was used to evaluate the second order and third order differentials, and the results [10] are as follows

$$\frac{\partial^2 B}{\partial z^2} \Big|_{z=0} = \frac{3\mu_0 I R^2}{2} \left\{ \frac{4z_0^2 - R^2}{\left[z_0^2 + R^2 \right]^{7/2}} + \frac{4z_0^2 - R^2}{\left[z_0^2 + R^2 \right]^{7/2}} \right\} \quad (13)$$

$$\frac{\partial^3 B}{\partial z^3} \Big|_{z=0} = \frac{15\mu_0 I R^2}{2} \quad (14)$$

From equations 13 and 14, one can note that the gradient field at the center of the loops is not entirely linear due to the presence of these higher order terms of the magnetic field expansion. As a result, the image is blurred. These higher order terms cannot be suppressed in a single Maxwell pair. Nevertheless, numerous ways have been developed to improve image quality by utilizing multiple pulse sequences [17, 18], and clever arrangement of gradient coils. In the following section, a method for creating a linear gradient for a multiple turn Maxwell pair is described.

Generating a linear gradient field using multiple Maxwell pairs

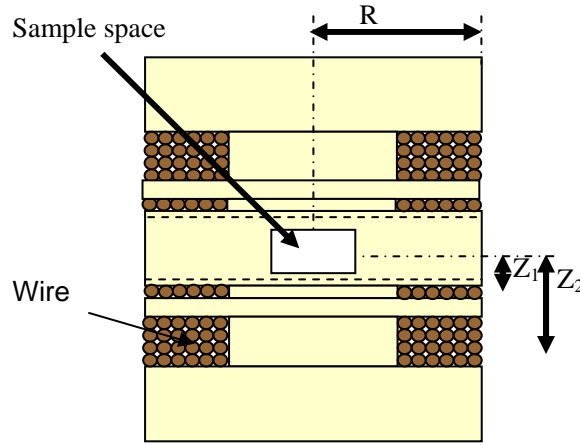


Figure 5: Not drawn to scale. This figure shows a cross section of a multiple turn Maxwell pair

In 1989, Suits and Wilkens developed a way to create a more linear gradient by eliminating the higher order terms of the magnetic field expansion [11]. They did this by reinforcing the following boundary conditions, which suppresses the higher order terms of the magnetic field expansion. A detailed derivation of this result can be found in [11]

$$Z_1 = 0.44R \quad Z_2 = 1.19R \quad \frac{S_2}{S_1} = 7.47 \quad (15)$$

Z_1 is the distance from the center of the sample space to the center of the first set of turns and R is the corresponding average radius of that set of turns. Z_2 is the distance from the center of the sample space to the center of the second set of turns, and R is the corresponding average radius of that set of turns. $\frac{S_2}{S_1}$ is the ratio of the second set of Maxwell pairs to the first set of Maxwell pairs.

The advantage of this design is that the gradient is stronger due to the presence more turns and a linear gradient is created across the sample. In addition to

the stronger and more linear gradient, another advantage is that Joule's heating is minimized. Zhang and Cory derived the temperature change in copper wires for a gradient coil of n Maxwell pairs, and an average diameter D with an applied voltage V [8]. For a gradient pulse of time Δt , the temperature change is

$$\Delta T = 0.055 \frac{V^2 \Delta t}{n^2 D^2} \quad (16)$$

It can be seen from equation 16 that Joule's heating is minimized because the temperature increase for a particular pulse time decreases as the number of Maxwell pairs and average diameter of the coil increases.

Inductance of the coil

Inductance is a very important parameter in coil design. This is because higher coil inductance results in longer gradient rise times which may cause distorted/defective gradient pulse areas. Another negative factor of large inductance is higher back EMF which results in unwanted high power dissipation in the circuit [10, 12]. Therefore, it is of utmost importance to minimize the inductance of the coil. It is well known that the inductance for a multiple turn coil scales as N^2 (where N is the number of turns or twice the Maxwell pairs) [12]. Even though the goal is to increase number of turns for stronger gradients, there is the drawback of higher inductance. Hence, for optimum results the parameters to minimize inductance while maximizing the gradient strength will have to be considered carefully. Below are equations that give the inductance for an air core coil [13]. It should be noted that the units for the respective inductance equations have been normalized such that L is already in Henry (H).

The equation below is for a multilayer coil surrounded by air with no dielectric in the middle. It is a good approximation of the inductance for the second set of turns.

$$L = \frac{0.02r^2N^2}{(6r + 9l + 10d) \times 10^6} \quad (17)$$

where r , N , l and d are the mean radius of coil, the number of turns, length of the coil windings, the depth (or thickness) of the turns, respectively. The below equation is for a spiral coil in air which is a good inductance approximation for the first set of turns

$$L = \frac{r^2N^2}{(2r + 2.8d) \times 10^6} \quad (18)$$

Parameters used in this design

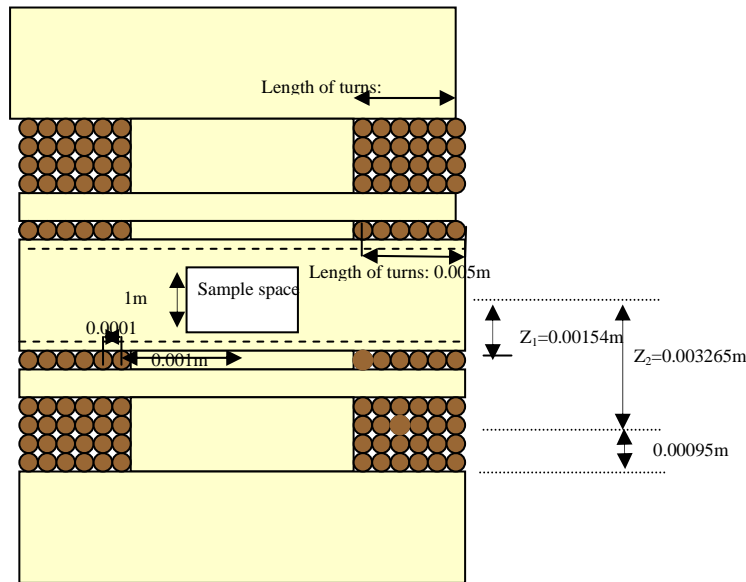


Figure 6: Not drawn to scale. The above set shows a labeled multiple turn Maxwell set with the exact parameters used in the design. The actual dimension of this set without turns is on the appendix page.

Having described the fundamental equations needed for gradient coils, the parameters used in this design will now be discussed. In order to generate a strong

gradient field we applied the principle of superposition of individual turns until a pulsed gradient of approximately 400, 000 G/cm is generated over a cubic millimeter.

The gradient equation for the first set of Maxwell turns is indicated below where we are summing the gradient contribution of each turn over all the turns:

$$G_1 = \sum_n \frac{3z\mu I}{\left(1 + \left(\frac{z}{R_n}\right)^2\right)^{5/2} R_n^3} \quad (19)$$

For the second set of Maxwell turns, we have to sum over R and z

$$G_2 = \sum_{n,m} \frac{3z\mu I}{\left(1 + \left(\frac{z_m}{R_n}\right)^2\right)^{5/2} R_n^3} \quad (20)$$

An excel spread sheet was used to calculate the total gradient field for the whole set.

The parameters, dimensions, and gradient for the whole multiple turn Maxwell set is indicated in the below table.

Current	I	200A
Permeability of free space	μ_0	$4\pi \times 10^{-7} \text{ N/m}$
Increments in radius horizontally (38 gauge wire)	R_n	0.0001m
Increments in radius vertically (38 gauge wire)	Z_n	0.0001m
Gradient field (55 turns)	G_1	124, 929.3G/cm
Gradient field (411 turns)	G_2	253, 106.6G/cm
Total gradient generated	$G_1 + G_2$	378, 035.9G/cm
Coil constant for the Set	$\frac{G}{I}$	1890.17G/Acm

Schematic of the gradient set with all of the dimensions included can be seen in the appendix section

The parameters for the inductance of the set are stated below. It should be noted that the effects of mutual inductance was neglected.

Mean radius of 1 st the coil	R	0.006m
No of turns for 1 st turns	N	55
Thickness of the turns of 1 st turns	D	0.005m
Self Inductance for first set of turns (calculated it for one side of the set)	L	761μH
Mean radius for second turns	R	0.0031m
Thickness for second turns	D	0.0021m
Number of second set of turns	N	411
Length of second turns	l	0.0019
Self Inductance for second set of turns (calculated it for one side of the set)	L	57.2μH

The temperature change of the turns for a pulse time of 100 μ s and a voltage of 50V is represented in the table below.

Pulse time	Δt	100 μ s
Voltage	V	50 volts
Number of Maxwell pairs	N	466
Diameter of coil	D	0.006m
Temperature change	ΔT	0.0017^oC

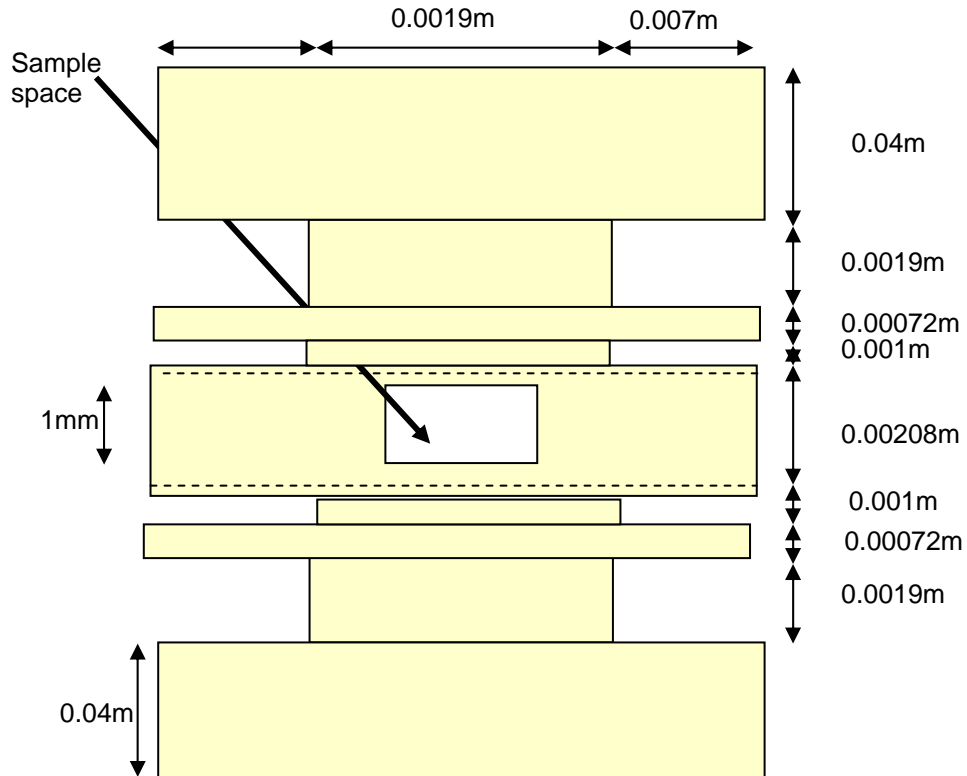
As seen from the table above, the temperature increase is substantially small for a long pulse time of 100 microseconds and large number of turns (466 Maxwell turns). This may be attributed to the larger surface area that the turns possess, which creates a thermal sink for rapid heat loss.

Conclusion

An analysis for generating gradients on the order of $\sim 400,000\text{G/cm}$ over 1mm^3 has been presented. Gradients of this magnitude will enable fine resolution in the nanometer regime. These gradient sets will be suitable for studying water transport and dynamics in various biopolymers. In the appendix of this thesis schematics are provided for building the device.

Appendix

Diagram A



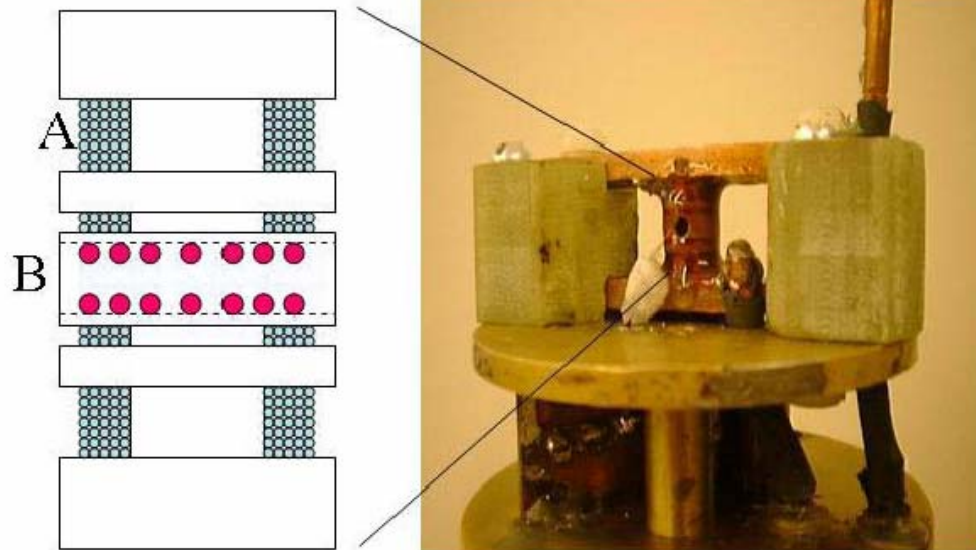
This figure shows a cross sectional view of the gradient for generating a field of 1890.17G/cmA

Diagram B



This picture shows an assembly of a solid state NMR apparatus in the lab at York. The cylindrical apparatus with a red and white triangular sticker is the device that generates the static magnetic field-B on the order of 4 Tesla, the cubical white device is a spectrometer, and the last is a computer which serves as an interface for controlling the system.

Diagram C



Gregory S. Boutis. Measurement of the spin rate of dipolar order in single crystal calcium fluoride. PhD Thesis, MIT (2002)

This picture shows what the gradient set will look like once completed. This device is usually engineered out of very strong material that can withstand the torques involved when the device is put into a strong magnetic field ($\sim 4\text{T}$).

Bibliography

1. Lauterbur PC, Image formation by induced local interactions: examples exploring Nuclear Magnetic Resonance. *Nature*, 242, (1973) 190-191
2. G. S. Boutis, D. Greenbaum, H. J. Cho, C. Ramanathan, D.G. Cory. "Spin Diffusion of two-spin correlated states in a dielectric crystal", *Physical Review Letters* 92, 13, 2004.
3. PT Callaghan. *Principles of Nuclear Magnetic Resonance Microscopy*. (Oxford Science Publications Press 1991)
4. Seung-Cheol Lee, Kiseong Kim, Junghyun Kim, Soonchil Lee, Jeong Han Yi, Sung Woo Kim, Kwon-Soo Ha and Chaejoon Cheong. One Micrometer Resolution NMR Microscopy, *Journal of Magnetic Resonance*, Volume 150, Issue 2, 2001, Pages 207-213
5. Xuio-wu Tang. *Nuclear Magnetic Resonance Microscopy*. PhD Thesis, MIT (1999)
6. C.P. Slichter. *Principles of Magnetic Resonance* (3rd edition, Springer-Verlag, Berlin Heidelberg New York, 1996)
7. A. Sodickson and D. Cory. A generalized k-space formalism for treating the spatial aspects of a variety of NMR experiments. *Progress in NMR spectroscopy* 33 (1998) 77-108
8. W. Zhang and D.G. Cory. Pulsed gradients NMR probes for solid state. *Journal of Magnetic Resonance*, 132, 144-149 (1998)
9. D. Griffiths, *Introduction to Electrodynamics* (Prentice Hall, New Jersey 1999)
10. J. Jin, *Electromagnetic Analysis and Design in Magnetic Resonance Imaging* (CRC Press, New York 1999)
11. B.H. Suits and D.E. Wilken. Improving magnetic field gradient coils for NMR imaging, *Journal of Physics E: Scientific Instruments*. 22 (1989) 565-573
12. R. Bowtell and P. Robyr. Multilayer Gradient Coil Design. *Journal of Magnetic Resonance* 131, 286-294 (1998)
13. <http://en.wikipedia.org/wiki/Inductor>. Accessed in May 2006.
14. Gregory S. Boutis. Measurement of the spin rate of a dipolar order in single crystal calcium fluoride. PhD Thesis, MIT (2002)
15. E. Fukushima and S. B. W. Roeder. *Experimental pulse NMR: A nuts and bolts application* (Westview press, Colorado, 1981)
16. L. Ciobanu, D. A. Seeber and C. H. Pennington, 3D MR microscopy with resolution 3.7 mm by 3.3 mm by 3.3 mm, *Journal of Magnetic Resonance*, Volume 158, Issues 1-2, 2002, Pages 178-182.
17. G.C. Chingas, J.B. Miller and A.N. NMR images of solids. *Journal of Magnetic Resonance*, 66 530-535 (1986)
18. A.N. Garroway, J Baun. M.G. Munowitz, A. Pines, NMR imaging in solids by multiple-quantum resonance. *Journal of Magnetic Resonance*, 60 337-341 (1984)